ELSEVIER

Thermochimica Acta 345 (2000) 3–12

thermochimica acta

www.elsevier.com/locate/tca

Thermal contact conductance in advanced AC calorimetry

Alexander A. Minakov*

General Physics Institute, Vavilov st. 38, 117942 Moscow, Russia

Received 13 July 1999; received in revised form 24 September 1999; accepted 26 September 1999

Abstract

The new capabilities of AC calorimetry, when working at frequencies above the classical (quasi-static) limit, were realized. The method of the Thermal-Waves-Transmission spectroscopy for simultaneous determination of the sample's heat capacity and thermal conductivity was developed on the basis of the advanced AC calorimetry technique. The idea of the method was to use the information about the phase and the amplitude of the thermal wave transmitted through a plate-like sample. The progress in the advanced technique was attained, when the thermal contact conductance was measured and taken into account. It was shown, that the Thermal-Waves-Transmission spectroscopy can be applied for various substances with thermal conductivity varied in the broad range 0.1–500 W/m K.

Keywords: Temperature-modulated calorimetry; Thermal conductivity; Thermal contact conductance; Thermal-Waves-Transmission spectroscopy; Dynamic heat capacity

1. Introduction

Investigation of phase transitions and relaxation phenomena in inorganic materials, polymers and biological objects is important for understanding their physics, as well as for providing practically valuable information on these substances. AC calorimetry is a powerful technique, which was successfully used for phase transitions investigation and time-dependent or frequency-dependent heat capacity measurements in condensed matter systems [1–13].

Recently, the new capabilities of AC calorimetry, when working at frequencies above classical limit, were demonstrated [12,13]. The advanced AC calorimetry was developed on the basis of the classical AC calorimetry technique. The idea of the method was to use the information about the phase and the amplitude of the temperature wave transmitted through a plate-like sample for simultaneous determination of the sample's heat capacity C_S and thermal conductivity λ_S. It was shown, that the AC calorimeter, described in [14,15], can be used at relatively high frequencies, when the temperature oscillations in the sample are not quasi-static. In this calorimeter an oscillating heat flow $P_0 \cos(\omega t)$ is supplied to one side of the sample, and the temperature oscillations $T_0 \sin(\omega t + \varphi)$ are measured on the other side. The two parameters, C_S and λ_S, can be determined from the two measured values, the amplitude T_0 and the phase φ of the transmitted temperature wave. The mathematical algorithm to do so was presented in the paper [12]. Moreover, using the information about the amplitudes T_{01} and T_{02} as well as the phases φ_1 and φ_2 on both sides of the sample, one can obtain simultaneously the complex heat capacity $\mathbf{C}_S(\omega)$ and the complex thermal

* Fax: +7-095-135-82-81.
E-mail address: minakov@ran.gpi.ru (A.A. Minakov).

0040-6031/00/$ – see front matter
PII: S0040-6031(99)00360-3

conductivity $\lambda_S(\omega)$, i.e. four parameters: $\mathrm{Re}(\mathbf{C}_S)$, $\mathrm{Im}(\mathbf{C}_S)$, $\mathrm{Re}(\lambda_S)$ and $\mathrm{Im}(\lambda_S)$. Thus, the improvement of classical AC calorimetry has brought up a novel method: Thermal-Waves-Transmission spectroscopy. Its physical mechanism is transmission of thermal waves through a sample.

The advanced AC calorimetry was successfully applied to studies of polymer materials [12,13]. The ideal thermal contact of the sample with the calorimeter cell was assumed in [12,13]. This approximation was sufficient for polymers — the materials with relatively low thermal conductivity. Usually, after first melting–crystallization cycle polymers provide a good and stable thermal contact due to nice adhesion with substrate. On the other hand, the thermal contact should be formed by a liquid-like material in the case, when the sample cannot be melted. The thermal conductance of a dry thermal contact is relatively low and irreproducible. This conductance depends on the ambient gas pressure as well as on the sample–substrate pressure. Thus, when dealing with solids, a good thermal contact can be made by forming a thin layer of some adhesive surfactant between the sample and substrate. The vacuum grease, apiezon, can be used for this purpose. The grease layer can be made with reproducible thickness. Furthermore, the relatively small temperature gradient in the thin grease layer can be neglected, provided a sample with low thermal conductivity, $\lambda_S < 1$ W/m K, is investigated. But this approximation cannot be applied for materials with higher thermal conductivity.

The aim of this work is to further advance an AC technique, taking into account the thermal contact conductance on the sample's faces. To focus on the thermal contact conductance, we consider only the case of the frequency independent sample's parameters C_S and λ_S. To determine the parameters C_S and λ_S simultaneously, it is sufficient to measure temperature modulation on one side of the sample, which is opposite to the heated sample's surface. It is noteworthy, that the method can be applied for the case of complex sample's parameters, provided temperature modulation amplitudes are measured on both sides of the sample.

In the next section we present the description of the physical principles of the method and the mathematical algorithm of C_S and λ_S calculations from the measured complex amplitude of the temperature modulation. The calibration of the calorimeter and the thermal contact conductance is described in the third section. The fourth section is devoted to the experimental investigation of the thermal contact reproducibility and the measurements linearity relative to the sample's thickness. In the fifth section the experimental results for materials with different thermal conductivity are presented. The errors of the method are considered in this section.

2. Description of the method

The calorimeter cell — the system for excitation and registration of temperature modulation in a disk-shaped sample — consists of a heater, a sensor, and a holder. The sample is placed between the heater and the sensor substrates, as it is shown in Fig. 1. Thin layers of vacuum grease (apiezon) are used for providing good thermal contacts at the sample's faces. The heater and the sensor are formed on the surfaces of polished sapphire disks of 3.0 mm diameter and of thickness 100 μm. The heater is a chromium film ca. 0.1 μm, sputtered on the first sapphire substrate. Copper contact pads are sputtered on the film, and copper wires of 50 μm diameter are welded to the pads. The power of the resistive heater equals $P_0(1 + \cos \omega t)$, where $\omega/2$ is the angular frequency of the electric current and P_0 the average power of the heater. To form the sensor, a copper film is sputtered on the second sapphire substrate. The thermocouple (Cu–Cu:Fe) wires of 50 μm diameter are welded to the copper film. The sensor is glued on a silk net, which serves as holder. Thus, the system consists of six layers, including sample and two grease layers.

This layered system is heated by uniform heat flow of oscillating rate $P = P_0 \cos(\omega t)$. The flow is applied to the outer face of the first layer at $z = 0$ and propagates through the system along z-axis. The cross-section area S of the system is independent on z. Provided the heat leakage through the periphery of the system is negligible, the plane thermal waves $T = \mathrm{Re}[T_0 \exp(\mathrm{i}\omega t \pm \mathbf{k}z)]$ propagate across the system, where $\mathbf{k} = \exp(\mathrm{i}\pi/4)(\omega c/\lambda)^{1/2}$, c, specific heat capacity and λ, thermal conductivity of the material. In other words $\mathbf{k} = (k + \mathrm{i}k)/\sqrt{2}$, where $k = (\omega c/\lambda)^{1/2}$. Thus, the wave number and the damping coefficient of these waves are equal to $k/\sqrt{2}$. Stationary oscillating

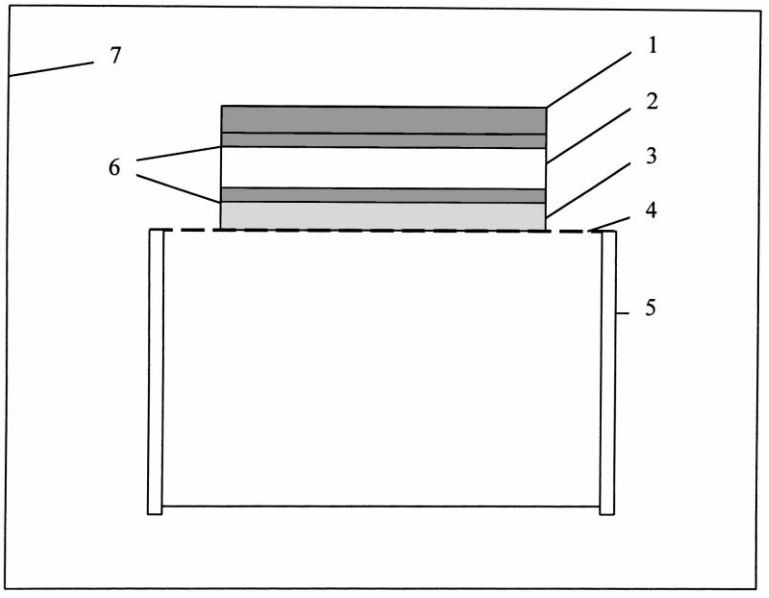

Fig. 1. Schematic cross-sectional view of the calorimeter cell. The heater 1, the sample 2 and the sensor 3 are fixed on the thin silk net 4, which is stretched on the cylinder holder 5. The thin grease layers 6 are formed for the stable heat contacts. The cell is put into the thermostat 7.

solution of the heat transfer equation without heat sources can be written as follows: $\mathrm{Re}\{\exp(\mathrm{i}\omega t)\ [\mathbf{a}\sinh(\mathbf{k}z) + \mathbf{b}\cosh(\mathbf{k}z)]\}$. Therefore the thermal wave $\mathbf{T}_i(z) = \exp(\mathrm{i}\omega t)\ \{\mathbf{a}_i \sinh\ [\mathbf{k}_i(z - \xi_\mathrm{i})] + \mathbf{b}_i \cosh\ [\mathbf{k}_i(z - \xi_\mathrm{i})]\}$ is excited in ith layer, where ξ_i the coordinate of ith boundary. The complex coefficients $\mathbf{a}_i$ and $\mathbf{b}_i$ are determined by boundary conditions for temperature and heat flow amplitudes on faces of ith layer. The amplitude and the phase of the thermal wave propagating through the sample is measured. The complex amplitude $\mathbf{T}_\mathrm{A}$ of the temperature modulation is measured on the surface between the sensor and the holder in the calorimeter considered in this paper.

In general, the following effective heat capacity is measured in classical AC calorimetry:

$$\mathbf{C}_\mathrm{eff} = P_0/(\mathrm{i}\omega\mathbf{T}_\mathrm{A}), \tag{1}$$

which is proportional to the heat-flow amplitude P_0 and inversely proportional to the measured complex amplitude $\mathbf{T}_\mathrm{A}$. Of course, at sufficiently low frequencies the effective heat capacity $\mathbf{C}_\mathrm{eff}$ equals the sum of the sample's heat capacity C_S and the heat capacity of the empty cell, provided the temperature modulation is quasi-adiabatic. The phase shift $\varphi = -\mathrm{Arg}\ (\mathbf{C}_\mathrm{eff})$ between the temperature modulations in the heater and in the sensor equals zero at these conditions. In fact, the phase shift between the heat-flow and $\mathbf{T}_\mathrm{A}$ equals $\varphi - \pi/2$. As the trivial phase lag $\pi/2$ is not of interest, we consider the phase shift φ between temperature modulations on the both sides of the system. At higher frequencies the relation between the measured $\mathbf{C}_\mathrm{eff}$ and C_S is complicated.

As it was shown in [12], provided the heat leakage into the wires of the thermocouple and through the periphery of the system is negligible, the measured $\mathbf{C}_\mathrm{eff}$ for the system consisting of n layers can be expressed as follows:

$$\mathbf{C}_\mathrm{eff} = \cosh(\boldsymbol{\alpha}_1)\cdots\cosh(\boldsymbol{\alpha}_{n-1})[C_1\tanh(\boldsymbol{\alpha}_1)/\boldsymbol{\alpha}_1 + \cdots + C_n\tanh(\boldsymbol{\alpha}_n)/\boldsymbol{\alpha}_n + G/\mathrm{i}\omega + \mathbf{B}], \tag{2}$$

where $\boldsymbol{\alpha}_i = \exp(\mathrm{i}\pi/4)\alpha_\mathrm{i}$; $\boldsymbol{\alpha}_i = d_i k_i$, the parameter characterizing the thermal length of the ith layer; d_i the thickness of the ith layer; C_i, heat capacity of the ith layer; G, ambient gas depending constant, characterizing the heat-link between the system and the thermostat. The cross terms are presented by the sum $\mathbf{B} = \mathbf{B}_3 + \mathbf{B}_5 + \cdots + \mathbf{B}_{2m+1}$, where $2m + 1 \leq n$.

Denote $\beta_{ab} = \lambda_a k_a/\lambda_b k_b$, then $\mathbf{B}_i$ can be written as follows:

$$\mathbf{B}_3 = \sum (C_a/\boldsymbol{\alpha}_a)\beta_{cb}\tanh(\boldsymbol{\alpha}_a)\tanh(\boldsymbol{\alpha}_b)\tanh(\boldsymbol{\alpha}_c), \quad (3)$$

$$\mathbf{B}_5 = \sum (C_a/\boldsymbol{\alpha}_a)\beta_{cb}\beta_{ed}\tanh(\boldsymbol{\alpha}_a)\tanh(\boldsymbol{\alpha}_b) \times \tanh(\boldsymbol{\alpha}_c)\tanh(\boldsymbol{\alpha}_d)\tanh(\boldsymbol{\alpha}_e),$$

and so on for all indexes, such as $a < b < c < d < e \ldots$ The sum $\mathbf{B}_3$ is taken over all combinations of three elements from n, i.e. over C_n^3 elements, $\mathbf{B}_5$-over all combinations of five elements from n, over C_n^5 elements, and so on. The cross terms are relatively small at sufficiently low frequencies. In fact, at low frequencies $\mathbf{B}_3$ decreases as ω and $\mathbf{B}_5$ as ω^2. Since, $\tanh(\alpha_i) \approx \alpha_i$ at small α_i, and $\alpha_i \sim \sqrt{\omega}$. It is noteworthy that the Eq. (2) was obtained in general case, when the sample's heat capacity and thermal conductivity can be complex.

Consider the Heater–Sample–Sensor–Holder system consisting of six layers, including two grease layers between sample and heater as well as between sample and sensor. Note that the heater and the sensor are formed on the equal sapphire substrates. That is why, we denote C_0 and d_0 the total heat capacity and the total thickness of two substrates, c_0 and λ_0 specific heat capacity and thermal conductivity of sapphire. Denote the parameters of the holder and of the grease layer in the same manner with subscripts 'h' and 'g'. In the case of six layers, at $n = 6$, the sum $\mathbf{B}$ in Eq. (2) equals $\mathbf{B}_3 + \mathbf{B}_5$, where $\mathbf{B}_3$ is the sum of 20 elements, and $\mathbf{B}_5$ the sum of six elements. Eqs. (2) and (3) can be simplified, if we take into account that the grease layer is relatively thin, d_g ca. 4 μm, and $C_g \ll C_0$. Thus, the terms from $\mathbf{B}_3$, which are proportional to β_{gi}, can be neglected, because $\alpha_g\beta_{gi}$ proportional to C_g. On the other hand, the terms from $\mathbf{B}_3$, which are proportional to β_{ig}, cannot be neglected. Note, that $\alpha_g\beta_{ig} = (i\omega \cdot C_i)/(K_g\alpha_I)$, where $K_g = S(\lambda_g/d_g)$ the thermal conductance of the grease layer. Denote $K_0 = S(\lambda_0/d_0)$ the thermal conductance of the sapphire substrates, $\tau_g = C_0/K_g$ and $\tau_0 = C_0/K_0$ the characteristic times of thermal relaxation in the system. In fact, at room temperatures τ_g ca. 10^{-2} s and τ_0 ca. 5×10^{-3} s. Thus, $\tau_g > \tau_0$ in spite of small thickness d_g.

Consider Eqs. (2) and (3) at modulation frequency $f = \omega/2\pi$ below 100 Hz, when $\alpha_g \ll 1$ and $\tanh(\alpha_g) \approx \alpha_g$. In this case, the cross terms from $\mathbf{B}_5$ can be neglected within 4% accuracy. In fact, the main term in the sum $\mathbf{B}_5$ is $(C_0/\alpha_0)\ \beta_{Sg}\ \beta_{h0}\tanh(\alpha_S)\tanh(\alpha_g)\ \tanh(\alpha_h)\ [\tanh(\alpha_0/2)]^2$, which is equal to $\varepsilon\ [C_S\tanh(\alpha_S)/\alpha_S]$, where $\varepsilon = (i\omega\tau_g)\ (i\omega\tau_0)\ (C_h/C_0)\ [\tanh(\alpha_h)/\alpha_h]\ [\tanh(\alpha_0/2)/\alpha_0]^2$ and $\varepsilon \ll 1$. Actually, this term can be neglected at any temperatures and frequencies below 100 Hz, provided the error ca. 4% is acceptable. Thus, only the cross terms from $\mathbf{B}_3$ are taken into account. Consider the cross terms $(C_a/\alpha_a)\ \beta_{cg}\tanh(\alpha_a)\ \tanh(\alpha_g)\ \tanh(\alpha_c)$, which cannot be neglected. These terms can be written as follows: $(i\omega/K_g)\ [C_a\tanh(\alpha_a)/\alpha_a]\ [C_c\tanh(\alpha_c)/\alpha_c]$. Then, the effective heat capacity for the Heater–Sample–Sensor–Holder system at modulation frequencies below 100 Hz can be expressed as follows:

$$\mathbf{C}_{eff} = \cosh(\boldsymbol{\alpha}_0)\cosh(\boldsymbol{\alpha}_s)\cosh(v\boldsymbol{\alpha}_g)[\mathbf{A}_0 + \mathbf{A}_h + vC_g + G/i\omega + \mathbf{S}_0 + \mathbf{S}_h], \quad (4)$$

$$\mathbf{A}_0 = [C_0\tanh(\boldsymbol{\alpha}_0)/\boldsymbol{\alpha}_0] \times [1 + (i\omega v\tau_g)\tanh(\boldsymbol{\alpha}_0/2)/\boldsymbol{\alpha}_0],$$

$$A_h = [C_h\tanh(\boldsymbol{\alpha}_h)/\boldsymbol{\alpha}_h][1 + (i\omega v\tau_g)\tanh(\boldsymbol{\alpha}_0)/\boldsymbol{\alpha}_0],$$

$$\mathbf{S}_0 = [C_S\tanh(\boldsymbol{\alpha}_S)/\boldsymbol{\alpha}_S]\{1 + (i\omega v\tau_g)\tanh(\boldsymbol{\alpha}_0)/\boldsymbol{\alpha}_0 + [(\beta_{0s})^2 - 1][\sinh(\boldsymbol{\alpha}_0/2)]^2/\cosh(\boldsymbol{\alpha}_0)\},$$

$$\mathbf{S}_h = [C_h\tanh(\boldsymbol{\alpha}_h)/\boldsymbol{\alpha}_h][(i\omega v\tau_{Sg})\tanh(\boldsymbol{\alpha}_S)/\boldsymbol{\alpha}_S + (\beta_{0S}/2 + \beta_{S0}/2)\tanh(\boldsymbol{\alpha}_0)\tanh(\boldsymbol{\alpha}_S)],$$

where $\tau_{Sg} = C_S K_g$, $v = 2$ the number of grease layers, $\beta_{S0} = 1/\beta_{0S}$ and $\beta_{0S} = (C_0\alpha_S/(C_S\alpha_0)$ by definition. Of course, the obvious relation $\mathbf{C}_{eff} \approx (C_0 + C_h + 2C_g + C_S + G/i\omega)$ follows from Eq. (4) at sufficiently low frequencies. In general, the two parameters C_S and α_S can be determined from the measured complex $\mathbf{C}_{eff}$, provided the other parameters in Eq. (4) are known. Finally, the thermal conductivity λ_S is determined from the following relation: $\lambda_S = \omega C_S d_S/S\alpha_S^2$.

3. Calibration of the calorimeter

Consider the effective heat capacity $\mathbf{C}_{emp}$ of the empty cell consisting of four layers. The expression for $\mathbf{C}_{emp}$ follows from Eq. (4) at $C_S = 0$, $\alpha_S = 0$ and $v = 1$:

$$\mathbf{C}_{emp} = \cosh(\alpha_0)\cosh(\alpha_g)[\mathbf{A}_0 + \mathbf{A}_h + C_g + G/i\omega]. \quad (5)$$

This is only the parameter G which depends on ambient gas pressure. But this dependence is very weak in the pressure range 1–100 Pa. In all measurements the nitrogen gas pressure was ca. 10 Pa and G was equal to 1.07 mW/K at 300 K. The cell parameters G, $\alpha_0/\sqrt{f}$, $\alpha_h/\sqrt{f}$, C_0, C_h, were determined in advance without a sample. It was found, that the thermal parameters of the grease layer, $\alpha_g/\sqrt{f}$, K_g and C_g, are related to the dimensionless parameter p, characterizing the thickness of the layer. The parameter p is defined as follows: $d_g = pd_{g0}$, where d_{g0} is the average grease-layer thickness, ca. 4 μm. This thickness was reproducible within 10% accuracy. Denote $p_0 = 1$ the average value of the parameter p, corresponding to the average thickness. The thermal parameters, $K_{g0} = 0.27 \pm 0.005$ W/K, $\alpha_{g0}/\sqrt{f} = 0.051 \pm 0.001$ $s^{1/2}$ and $C_{g0} = 0.07 \pm 0.005$ mJ/K, of the average grease layer at 300 K were determined from the measurements for the empty cell and for multilayered systems with equivalent sapphire samples. In general, $K_g = (1/p)\cdot 0.27$ W/K, $\alpha_g/\sqrt{f} = p$ 0.051 $s^{1/2}$ and $C_g = p$ 0.07 mJ/K.

Thus, we have six parameters, G, $\alpha_0/\sqrt{f}$, $\alpha_h/\sqrt{f}$, C_0, C_h and p, for fitting the experimental dependency $\mathbf{C}_{emp}(T, f)$ by Eq. (5) at any fixed temperature in the broad frequency range 0.1–100 Hz. The experimental dependencies of the absolute value C_{emp}(300 K, f) and of the phase shift $\varphi = -\mathrm{Arg}(\mathbf{C}_{emp})$ for a normal and a relatively thin grease layers are shown in Fig. 2. These experimental curves are well described by Eq. (5) in the frequency range 0.1–100 Hz at the following parameters: $C_0 = 4.3$ mJ/K, $C_h = 2.05$ mJ/K, $\alpha_0/\sqrt{f} = 0.17$ $s^{1/2}$, $\alpha_h/\sqrt{f} = 2.19$ $s^{1/2}$, $G = 1.07$ mW/K with $p = 0.95$ for the first curve and $p = 0.70$ for the second. These calibration parameters were determined within 2% accuracy. To illustrate the influence of the thermal contact conductance, the curves, calculated for the ideal thermal contact ($p = 0$), are shown by dashed lines. As shown in Fig. 2, the thermal contact conductance has no effect on C_{emp}(300 K, f) at frequencies below 10 Hz, but this effect is essential at ca. 100 Hz.

Once the cell calibration is performed, the described algorithm makes it possible to carry out simultaneous measurements of the sample's heat capacity and thermal conductivity. The measurements of $\mathbf{C}_{eff}$ vs. frequency were performed at constant heat-flow amplitude P_0. Depending on the sample's heat capacity, P_0 was varied in the range 6–20 mW so as the temperature–modulation amplitude T_A to be approximately the same for samples with different mass. Indeed, the amplitude T_A was decreased with frequency at constant P_0. In all experiments the amplitude T_A was changed in the range from 1 to

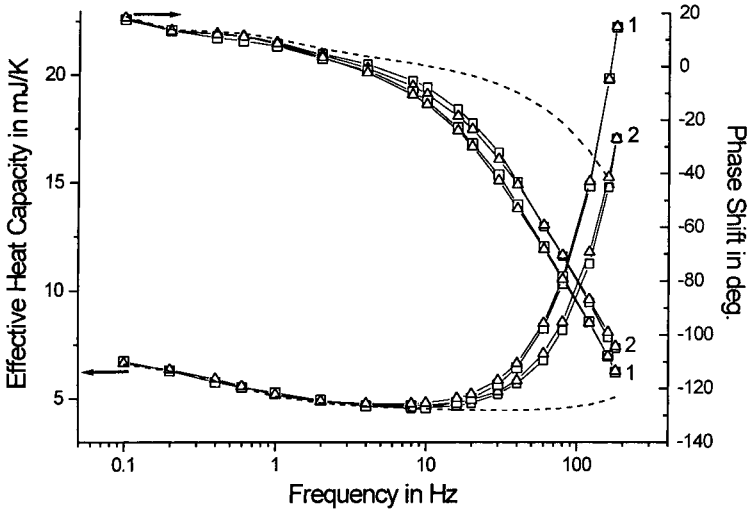

Fig. 2. Frequency dependences of measured (squares) and calculated (triangles) effective heat capacity C_{emp}(300 K) and phase shift $\varphi = -\mathrm{Arg}(\mathbf{C}_{emp})$ for empty cell: 1, for the normal grease layer with the thickness parameter $p = 0.95$; and 2, for relatively thin layer with $p = 0.70$. The dashed lines show the dependences for the ideal thermal contact with $p = 0$.

10^{-3} K with frequency variation in the range 0.1–100 Hz.

4. Thermal contact reproducibility and measurements linearity

Further, we check the reproducibility of the thermal contact conductance and of the measurements linearity relative to the sample's thickness. Consider the results obtained for a set of identical samples. The samples, received from ''Kristallhandel Keplin'', were polished sapphire disks of 3.0 ± 0.01 mm diameter and of thickness $d_S = 110 \pm 5$ μm. The disks were cut out in *C*-plane of a sapphire single crystal. All parameters of these disks were the same as of the cell-substrates, except thickness. Note, that the thickness of one cell-substrate equals $d_0/2 = 100$ μm. Therefore, the sample's parameters were known from the previous measurements: $C_S = 0.55 \times C_0$ and $\alpha_S/\sqrt{f} = 0.55\ \alpha_0/\sqrt{f}$.

These parameters correspond to the specific heat capacity $c_S = (3.0 \pm 0.1) \times 10^6$ J/m^3 K and the thermal conductivity $\lambda_S = 27 \pm 1$ W/m K at 300 K. The error ca. 5% in the sample's thickness leads to the 5% uncertainty in c_S and λ_S. In this case, other 2% uncertainties in the calibration parameters, C_0 and $\alpha_0/\sqrt{f}$, are insignificant. The specific heat capacity is in agreement with the data available in the Handbooks [16–19] for sapphire at 300 K: $c = (2.99–3.09) \times 10^6$ J/m^3 K with the density $\rho = 3970–3985$ kg/m^3 and the molecular weight $\mu = 101.96$. The thermal conductivity $\lambda_S = 27$ W/m K is smaller than the value $\lambda = 35$ W/m K along *C*-axis at 273 K, which is presented in [16] for a bulk sapphire. Our results, obtained for the thin sapphire substrates, are in agreement with the data presented in [17] for the analogous thin sample: $\lambda = 25.1$ W/m K, $d = 100$ μm at 300 K. Due to mechanical treatment, the sample structure is disturbed near the polished faces. This may be the reason of the relatively small sample's thermal conductance. The parameters of the all samples in the following experiment were the same.

The experimental dependencies of $C_{eff}(300\ K, f)$ and the phase shifts $\varphi = -\mathrm{Arg}(\mathbf{C}_{eff})$ for one, two and three sapphire samples as well as for the empty cell are shown in Fig. 3. These experimental curves are well described by Eq. (4) in the frequency range 0.1–100 Hz with the following parameters: $C_S = n\ (d_S/d_0)\ C_0$, $\alpha_S = n\ (d_S/d_0)\ \alpha_0$ and $v = n + 1$, where $n = 0, 1, 2, 3$ is the number of sapphire samples in the cell; v, the number of the grease layers. The grease thickness parameter p was as follows: $p = 0.95$ for the empty cell, $p = 1.00$ for one sapphire sample, $p = 1.10$ for

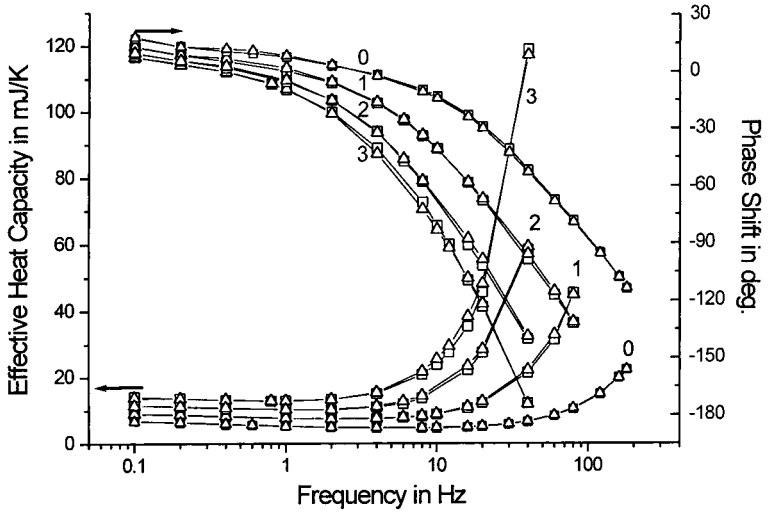

Fig. 3. Frequency dependences of measured (squares) and calculated (triangles) effective heat capacity $C_{eff}(300\ K)$ and phase shift $\varphi = -\mathrm{Arg}(\mathbf{C}_{eff})$; 0, for the empty cell; 1, for one sapphire sample in the cell; 2, two identical sapphire samples in the cell; and 3, three samples in the cell. The parameters of the grease layer thickness were as follows: $p = 0.95$, 1.00, 1.10, 1.01, correspondingly.

two samples and $p = 1.01$ for three samples. Thus, the grease layer thickness is reproducible within 10% accuracy. It is shown, the experimental results for sapphire thermal parameters, c_S and λ_S, are independent on the number of samples in the cell, that is on the sample's thickness.

5. Experimental results for various materials and accuracy

Once the thermal contact conductance is taken into account, the thermal parameters of materials with relatively high thermal conductivity can be measured. Consider the experimental results for a copper monocrystalline sample. The sample was the polished disk of 3.1 ± 0.05 mm diameter and 500 ± 10 μm thickness. Thus, the uncertainty in the sample's faces area was ca. 3% and in the volume ca. 4%. The frequency dependences of measured and calculated effective heat capacity $C_{eff}(300\ K)$ and of the phase shift $\varphi = -\mathrm{Arg}(\mathbf{C}_{eff})$ for this sample are shown in Fig. 4. The experimental curves are well described by Eq. (4) in the frequency range 0.1–100 Hz at the following parameters: $C_S = 12.9 \pm 0.1$ mJ/K, $\alpha_S/\sqrt{f} = 0.113 \pm 0.005\ s^{1/2}$ and $p = 1.15 \pm 0.05$. These results correspond to the following sample's parameters: $c_S = (3.4 \pm 0.1) \times 10^6$ J/m^3 K and $\lambda_S = 420 \pm 25$ W/m K at 300 K. The uncertainty ca. 4% in the sample's volume leads to 4% error in c_S. The uncertainty in λ_S ca. 6% arises due to 5% error in the parameter α_S and 3% error in the sample's faces area. These c_S and λ_S are in agreement with the data available in the Handbooks [16–19]: $\lambda = 400$–420 W/m K, density $\rho = 8960$ kg/m^3, molecular weight $\mu = 63.55$, and $c = 384$–386 J/kg K, i.e., $c = (3.44$–$3.46) \times 10^6$ J/m^3 K at 300 K.

The relative error of the effective heat capacity fitting, $\delta C_{eff} = \Delta C_{eff}/C_{eff}$, and the absolute error of the phase shift fitting, $\Delta\varphi$, are shown in Fig. 4. The increase of the errors δC_{eff} and $\Delta\varphi$ with the frequency can be attributed to the fact, that the cross terms from the sum $\mathbf{B}_5$ were neglected. The fluctuations of the measured $\mathbf{C}_{eff}$ around the mean value are increased with the frequency also. This growth of the fluctuations is attributed to the reduction of T_A and of the

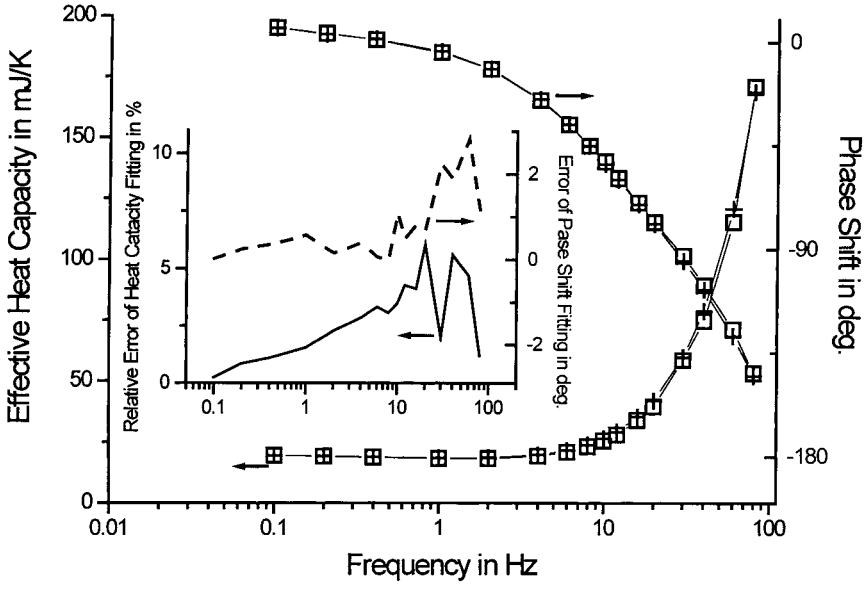

Fig. 4. Frequency dependences of measured (squares) and calculated (crosses) effective heat capacity $C_{eff}(300\ K)$ and phase shift $\varphi = -\mathrm{Arg}(\mathbf{C}_{eff})$ for single-crystalline copper disk of diameter 3.1 mm and thickness 0.50 mm. The curves correspond to the following sample's parameters: $c_S = (3.4 \pm 0.1) \times 10^6$ J/m^3 K and $\lambda_S = 420 \pm 25$ W/m K. The relative error of the effective heat capacity fitting, δC_{eff}, and the absolute error of the phase shift fitting, $\Delta\varphi$, are shown in the insert.

measured signal with the frequency at constant P_0. It is noteworthy that the parameter C_S can be determined from the low-frequency part of $C_{eff}(f)$ dependence directly, where the error $\delta C_{eff} < 2\%$. On the other hand, the parameter $\alpha_S/\sqrt{f}$ is determined from the high-frequency part of the curves $\varphi(f)$ and $C_{eff}(f)$, where the error in the curves fitting reaches 5%. Therefore, the heat capacity C_S is determined within 2% accuracy and the thermal conductivity λ_S within 5% accuracy.

To show the difference between the following dependences: $\mathbf{C}_{eff}(C_S)$, $\mathbf{C}_{eff}(\alpha_S)$, and $\mathbf{C}_{eff}(p)$, consider the complex derivatives $\partial\mathbf{C}_{eff}/\partial C_S$, $\partial\mathbf{C}_{eff}/\partial\alpha_S$, $\partial\mathbf{C}_{eff}/\partial p$. The relative variations of the effective heat capacity $\mathbf{C}_{eff}$ at 1% changes of C_S, α_S, and p are equal to the following relations: C_{eff}^{-1} $(\partial\mathbf{C}_{eff}/\partial C_S)$ $(0.01\ C_S)$, C_{eff}^{-1} $(\partial\mathbf{C}_{eff}/\partial\alpha_S)$ $(0.01\ \alpha_S)$, and C_{eff}^{-1} $(\partial\mathbf{C}_{eff}/\partial p)$ $(0.01\ p)$. The frequency dependences of C_{eff} and φ variations at 1% changes of C_S, α_S and p are shown in Fig. 5. The curves were calculated for a sample of 3 mm diameter, 0.3 mm thickness, $C_S = 7$ mJ/K, $\lambda_S = 10$ W/m K and for the same cell parameters as in Section 3. As it is shown in Fig. 5, the low frequency variation of C_{eff} is related mainly to the change of C_S. Thus, the value of C_S can be determined from the low frequency part of $C_{eff}(f)$ curve. At high frequencies the effective heat capacity C_{eff} depends strongly on the parameters α_S and p. The phase shift φ depends on α_S and p at all frequencies. The variation of C_S has very small influence on φ. Therefore, the parameters α_S and p can be determined from the shape of the curve $C_{eff}(f)$ at high frequencies and from the curve $\varphi(f)$ in the whole frequency range.

The measurements similar to the previous experiment were performed for a nickel monocrystalline sample. The sample was the roughly grinded disk of 3.1 ± 0.02 mm diameter and 310 ± 10 μm thickness. The experimental curves were well described by Eq. (4) at the following parameters: $C_S = 9.1 \pm 0.1$ mJ/K, $\alpha_S/\sqrt{f} = 0.285 \pm 0.015\ s^{1/2}$ and $p = 1.75 \pm 0.1$ at 300 K. The parameter p was relatively large because of rough surface treatment with 10 μm diamond paste. The results correspond to the following sample's thermal parameters: $c_S = (3.9 \pm 0.1) \times 10^6$ J/m^3 K and $\lambda_S = 29 \pm 2$ W/m K at 300 K. The uncertainty ca. 3% in the sample's volume leads to 3% error in c_S. The uncertainty in λ_S ca. 6% arises due to 5% error in the parameter α_S and 3% error in the sample's thickness. These values, c_S and λ_S, are in agreement with the data available in the Handbooks [16–19]: $c = 440$–

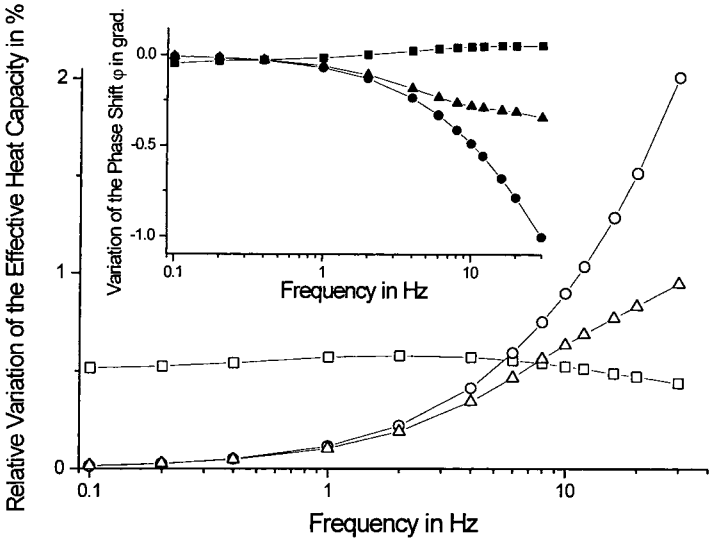

Fig. 5. Frequency dependences of the variations of the effective heat capacity value at 1% changes of the sample's heat capacity C_S (squares), of the parameter α_S (circles), and the parameter p (triangles). The corresponding dependences of the phase shift variations are shown in the insert. The curves were calculated for a sample of 3 mm diameter, 0.3 mm thickness, $C_S = 7$ mJ/K, $\lambda_S = 10$ W/m K and the same cell parameters as in Section 3.

444 J/kg K at 300 K with $\mu = 58.69$ and $\rho = 8900$ kg/m^3, i.e., $c = (3.92–3.95) \times 10^6$ J/m^3 K. The thermal conductivity of Ni is dependent on mechanical treatment and purity. As follows from [16–19], the value of λ_S can be in the range 20–90 W/m K at 300 K.

Finally, consider the possibility of $C_S(T)$ and $\lambda_S(T)$ measurements at a fixed frequency. In this case, the parameters λ_S and p cannot be determined separately. Assume, that the parameter p is equal to the average value $p_0 = 1$ within 10% accuracy. Then, the parameters $C_S(T)$ and $\lambda_S(T)$ can be calculated from the measured $\mathbf{C}_{eff}$ at a fixed frequency according to Eq. (4) at $p = p_0$. The uncertainty of the parameter p leads to the error in the measured thermal conductivity. This error depends on the sample's thermal conductivity. The smaller the thermal conductivity λ_S, the smaller the relative error $\delta\lambda_S = \Delta\lambda_S/\lambda_S$ at the same uncertainty of p. The relation between $\delta\lambda_S$ and δp can be find from Eq. (4) by fitting $\mathbf{C}_{eff}(f, \alpha_S + \delta\alpha_S, p_0)$ to $\mathbf{C}_{eff}(f, \alpha_S, p_0 + \delta p)$ at a fixed frequency. The error $\delta\lambda_S$ is related to the error $\delta\alpha_S$. Thus, we find the following relation between $\delta\lambda_S$ and δp at different λ_S: $\delta\lambda_S = 2.5\%$ at $\lambda_S = 1$ W/m K, $\delta\lambda_S = 5\%$ at $\lambda_S = 10$ W/m K, $\delta\lambda_S$ ca. 100% at $\lambda_S = 500$ W/m K, when δp ca. 10%, and $\delta\lambda_S = 30\%$ at $\lambda_S = 500$ W/m K, when $\delta p = 5\%$. Therefore, the temperature dependencies $C_S(T)$ and $\lambda_S(T)$ of the materials with λ_S ca. 10 W/m K can be measured simultaneously at a fixed frequency, provided the uncertainty of the thermal contact conductance is not too large. The approximation of the average thermal contact conductance cannot be applied for materials with large thermal conductivity λ_S ca. 100 W/m K. In this case, the measurements at different frequencies are impossible.

6. Conclusions

The method of the Thermal-Waves-Transmission spectroscopy for simultaneous determination of the sample's heat capacity and thermal conductivity is developed on the basis of the advanced AC calorimetry technique. The idea of the method is to use the information about the phase and the amplitude of the thermal wave transmitted through a plate-like sample. For the correct application of the method in an experimental set up, it was necessary to study the problem of a plane-thermal-wave transmission through a plate-like multilayered system. This problem was solved analytically for a wide range of experimental conditions. It was shown that the Thermal-Waves-Transmission spectroscopy can be successfully applied for simultaneous measurements of heat capacity and thermal conductivity of various materials with thermal conductivity varied in the broad range, provided the thermal contact conductance on the sample's faces is taken into account. The algorithm how to calculate the sample's thermal properties from the measured effective heat capacity is developed. It was shown that the approximation of the ideal thermal contact conductance can be applied only for materials with low thermal conductivity $\lambda_S < 1$ W/m K. The approximation of the average thermal contact conductance, $p = p_0$, can be applied for materials with intermediate thermal conductivity $\lambda_S \leq 10$ W/m K. The thermal properties of the materials with high thermal conductivity, λ_S ca. 100 W/m K, can be obtained from the frequency dependency of the effective heat capacity, measured in the broad frequency range 0.1–100 Hz. The linearity of the measurements relative to the sample's thickness was proved. The method can be easily generalized for the case of complex sample's thermal parameters, provided the temperature–modulation amplitudes on both sides of the sample are measured.

Acknowledgements

The author is grateful to Professor I. Hatta for stimulated discussions and comments to the manuscript. The financial support of the European Commission, grant number IC15CT96-0821, is gratefully acknowledged.

References

[1] P.F. Sullivan, G. Seidel, Phys. Rev. 173 (1968) 679.
[2] P. Handler, D.E. Mapother, M. Rayl, Phys. Rev. Lett. 19 (1967) 356.
[3] M.B. Salamon, Phys. Rev. B 2 (1970) 214.
[4] I. Hatta, A. Ikushima, J. Phys. Chem. Solids 34 (1973) 57.
[5] I. Hatta, Y. Nagai, T. Nakayama, S. Imaizumi, J. Phys. Soc. Jpn. 52 (Suppl. 47) (1983).
[6] I. Hatta, Y. Nagai, Mol. Cryst. Liq. Cryst. 123 (1985) 295.
[7] I. Hatta, Thermochim. Acta 304/305 (1997) 27.

[8] K. Ema, H. Yao, Thermochim. Acta 304/305 (1997) 157.
[9] Y. Saruyama, Thermochim. Acta 304/305 (1997) 171.
[10] M. Castro, J.A. Puertolas, Thermochim. Acta 304/305 (1997) 291.
[11] D. Finotello, S. Qian, G.S. Iannacchione, Thermochim. Acta 304/305 (1997) 303.
[12] A.A. Minakov, Yu.V. Bugoslavsky, C. Schick, Thermochim. Acta 317 (1998) 117.
[13] A.A. Minakov, C. Schick, Thermochim. Acta 330 (1999) 109.
[14] A.A. Minakov, O.V. Ershov, Cryogenics, 34 (ICEC Suppl.) (1994) 461.
[15] A.A. Minakov, Thermochim. Acta 304/305 (1997) 165.
[16] D.R. Lide, CRC Handbook of Chemistry and Physics, 79th ed., CRC Press, Boca Raton, FL, 1998–1999.
[17] I.G. Kozhevnikov, L.A. Novitskii, Therm.-Phys. Properties of Materials at Low Tempr., Moscow, 1982.
[18] I.K. Kikoin, Tables of Physical Values, Moscow, 1976.
[19] I.S. Grigoriev, E.Z. Meilikhov, Physical Values, Moscow, 1991.